REPORT DOCUMENTATION PAGE

Form Approved OMB NO. 0704-0188

1. REPORT DATE (DD-MM-YYYY)	2. REPORT TYPE	3. DATES COVERED (From - To)
	New Reprint	-

4. TITLE AND SUBTITLE

Conduction- and Valence-Band Energies in Bulk InAs1-x Sb x and Type II InAs1-x Sb x /InAs Strained-Layer Superlattices

5a. CONTRACT NUMBER

W911NF-12-2-0057

5b. GRANT NUMBER

5c. PROGRAM ELEMENT NUMBER

611102

6. AUTHORS

Youxi Lin, Ding Wang, Dmitry Donetsky, Leon Shterengas, Gela Kipshidze, Gregory Belenky, Stefan P. Svensson, Wendy L. Sarney, Harry S. Hier

5d. PROJECT NUMBER

5e. TASK NUMBER

5f. WORK UNIT NUMBER

7. PERFORMING ORGANIZATION NAMES AND ADDRESSES

Research Foundation of SUNY at Stony Brook U
Office of Sponsored Programs
W-5510 Melville Library
Stony Brook, NY 11794 -3362

8. PERFORMING ORGANIZATION REPORT NUMBER

9. SPONSORING/MONITORING AGENCY NAME(S) AND ADDRESS(ES)

U.S. Army Research Office
P.O. Box 12211
Research Triangle Park, NC 27709-2211

10. SPONSOR/MONITOR'S ACRONYM(S)

ARO

11. SPONSOR/MONITOR'S REPORT NUMBER(S)

62447-EL.8

12. DISTRIBUTION AVAILIBILITY STATEMENT

Approved for public release; distribution is unlimited.

13. SUPPLEMENTARY NOTES

The views, opinions and/or findings contained in this report are those of the author(s) and should not contrued as an official Department of the Army position, policy or decision, unless so designated by other documentation.

14. ABSTRACT

The energy gaps were studied in two types of structures: unrelaxed bulk In- As1-xSbx layers with x = 0.2 to 0.46 grown on metamorphic buffers and type II InAs1-xSbx/InAs strained-layer superlattices (SLS) with x = 0.225 to 0.296 in the temperature range from T = 13 K to 300 K. All structures were grown on GaSb substrates. The longest wavelength of photoluminescence (PL) at low temperatures was observed from bulk InAs0.56Sb0.44 with a peak at 10.3 um and full-width at half-maximum (FWHM) of 11 meV. The PL data for the bulk InAs1-xSbx materials of

15. SUBJECT TERMS

InAsSb, SLS, energy-band offsets, bowing, broadening

16. SECURITY CLASSIFICATION OF:			17. LIMITATION OF ABSTRACT	15. NUMBER OF PAGES	19a. NAME OF RESPONSIBLE PERSON
a. REPORT	b. ABSTRACT	c. THIS PAGE			Gregory Belenky
UU	UU	UU	UU		19b. TELEPHONE NUMBER: 631-632-8397

Report Title

Conduction- and Valence-Band Energies in Bulk InAs1-x Sb x and Type II InAs1-x Sb x /InAs Strained-Layer Superlattices

ABSTRACT

The energy gaps were studied in two types of structures: unrelaxed bulk In- As1-xSbx layers with x = 0.2 to 0.46 grown on metamorphic buffers and type II InAs1-xSbx/InAs strained-layer superlattices (SLS) with x = 0.225 to 0.296 in the temperature range from T = 13 K to 300 K. All structures were grown on GaSb substrates. The longest wavelength of photoluminescence (PL) at low temperatures was observed from bulk InAs0.56Sb0.44 with a peak at 10.3 um and full-width at half-maximum (FWHM) of 11 meV. The PL data for the bulk InAs1-xSbx materials of various compositions imply an energy gap bowing parameter of 0.87 eV. A low-temperature PL peak at 9.1 um with FWHM of 13 meV was observed for InAs0.704Sb0.296/InAs SLS. The PL spectrum of InAs0.775Sb0.225/InAs SLS under pulsed excitation revealed a second peak associated with recombination of electrons in the three-dimensional (3D) continuum with holes in the InAs0.775Sb0.225. This experiment determined the conduction-band offset in the InAs0.775Sb0.225/InAs SLS. The energies of the conduction and valence bands in unstrained InAs1-xSbx and their bowing with respect to the Sb composition are discussed.

REPORT DOCUMENTATION PAGE (SF298)
(Continuation Sheet)

Continuation for Block 13

ARO Report Number 62447.8-EL
Conduction- and Valence-Band Energies in Bulk ...

Block 13: Supplementary Note

Approved for public release; distribution is unlimited.

Journal of ELECTRONIC MATERIALS, Vol. 42, No. 5, 2013
DOI: 10.1007/s11664-013-2528-9

Conduction- and Valence-Band Energies in Bulk $InAs_{1-x}Sb_x$ and Type II $InAs_{1-x}Sb_x$/InAs Strained-Layer Superlattices

YOUXI LIN,[1,3] DING WANG,[1] DMITRY DONETSKY,[1] LEON SHTERENGAS,[1] GELA KIPSHIDZE,[1] GREGORY BELENKY,[1] STEFAN P. SVENSSON,[2] WENDY L. SARNEY,[2] and HARRY S. HIER[2]

1.—Department of ECE, Stony Brook University, Stony BrookNY 11794, USA. 2.—Army Research Laboratory, AdelphiMD 20783, USA. 3.—e-mail: youxi.lin@stonybrook.edu

The energy gaps were studied in two types of structures: unrelaxed bulk $InAs_{1-x}Sb_x$ layers with x = 0.2 to 0.46 grown on metamorphic buffers and type II $InAs_{1-x}Sb_x$/InAs strained-layer superlattices (SLS) with x = 0.225 to 0.296 in the temperature range from T = 13 K to 300 K. All structures were grown on GaSb substrates. The longest wavelength of photoluminescence (PL) at low temperatures was observed from bulk $InAs_{0.56}Sb_{0.44}$ with a peak at 10.3 μm and full-width at half-maximum (FWHM) of 11 meV. The PL data for the bulk $InAs_{1-x}Sb_x$ materials of various compositions imply an energy gap bowing parameter of 0.87 eV. A low-temperature PL peak at 9.1 μm with FWHM of 13 meV was observed for $InAs_{0.704}Sb_{0.296}$/InAs SLS. The PL spectrum of $InAs_{0.775}Sb_{0.225}$/InAs SLS under pulsed excitation revealed a second peak associated with recombination of electrons in the three-dimensional (3D) continuum with holes in the $InAs_{0.775}Sb_{0.225}$. This experiment determined the conduction-band offset in the $InAs_{0.775}Sb_{0.225}$/InAs SLS. The energies of the conduction and valence bands in unstrained $InAs_{1-x}Sb_x$ and their bowing with respect to the Sb composition are discussed.

Key words: InAsSb, SLS, energy-band offsets, bowing, broadening

INTRODUCTION

Development of bulk InAsSb alloys and InAsSb/InAs SLS with narrow energy gaps is attractive due to the possibility of photon generation and detection in the midwave and longwave infrared wavelength ranges.[1–8] Interest in these materials has increased in recent years.[9–21] One of the reasons is the prediction[17] and demonstration[18–20] of long carrier lifetimes in both bulk InAsSb and InAsSb/InAs SLS grown by molecular-beam epitaxy (MBE). The absence of Ga and the associated carrier recombination centers likely explain the relatively long carrier lifetime in InAsSb-based materials compared with InAs/GaSb-based SLS. Accurate predictions of the conduction- and valence-band energies and heterobarrier offsets are critically important for the design of barrier photodetectors with low dark currents.

In the case of bulk InAsSb alloys with high Sb compositions, the lattice mismatch of the epitaxial layer with the available substrates was accommodated with various types of buffer layers.[2–7,18,21] The buffer design and growth conditions can have a profound effect on the energy gaps of InAsSb alloys due to effects of residual strain, the possibility of Cu-Pt ordering,[7] and strain relaxation, which can explain the variation of the reported energy gaps for a given composition.

In previous works we reported PL and optical absorption spectra of unrelaxed unstrained bulk InAsSb grown on compositionally graded AlInAsSb or GaInSb buffers on GaSb substrates.[18,21] In this work, PL spectra were obtained for structures with AlInAsSb buffers of both newly grown and previously studied materials[18] in the temperature range extending up to 300 K and down to 20 K and under

(Received October 16, 2012; accepted February 5, 2013; published online March 8, 2013)

excitation power density as low as 2 W/cm^2. The additional data on the dependence of the energy gap on the bulk InAsSb composition resulted in an energy gap bowing parameter of 0.87 eV. The temperature dependences of the energy gaps for bulk $InAs_{0.8}Sb_{0.2}$ and $InAs_{0.56}Sb_{0.44}$ were determined from PL spectra, accounting for thermal broadening. The Varshni parameters for bulk InAsSb alloys were found to be $\alpha = 3.2 \times 10^{-4}$ eV/K and $\beta = 100.3$ K for Sb composition of 20% and $\alpha = 1.2 \times 10^{-4}$ eV/K and $\beta = 33.4$ K for Sb composition of 44%.

The PL spectra from $InAs_{1-x}Sb_x$/InAs SLS with Sb compositions from $x = 0.225$ to 0.296 were measured in the temperature range from 13 K to 150 K. The parameters of the SLS were close to those described in Ref. 19. The PL energies suggest a negative bowing of the valence band of InAsSb, similar to that observed in Refs. 9,10,24. Study of the PL spectra of $InAs_{0.775}Sb_{0.225}$/InAs SLS under pulsed pumping revealed a second peak at higher photon energy in addition to the main peak observed under continuous-wave excitation. The high-energy peak was attributed to transitions from the 3D continuum in the conduction band to quasi-two-dimensional (2D) states in the valence band of InAsSb. Accounting for the energy shift with strain and quantization allowed for the determination of the conduction-band offset at the $InAs_{0.775}Sb_{0.225}$/InAs interface. The energies of the conduction and valence bands in unstrained InAsSb with respect to InAs were determined for the range of Sb compositions in the studied SLS structures. The fit of the dependence of the valence-band energy of unstrained $InAs_{1-x}Sb_x$ on the composition x with a constant bowing parameter suggests a value of −0.3 eV for the valence-band bowing parameter, leaving +0.57 eV for the bowing parameter in the conduction band.

STRUCTURES

Bulk InAsSb epilayers on metamorphic buffers and InAsSb/InAs strained-layer superlattices (SLS) were grown on GaSb substrates by solid-source MBE. In the case of the bulk InAsSb materials, the lattice mismatch with the substrate was accommodated with compositionally graded AlInAsSb buffers.[18] During epitaxial growth, the topmost portion of the buffer remained unrelaxed under a residual strain, with almost complete relaxation occurring in the lower portion of the grade, beginning at the interface with the substrate. Transmission electron microscopy (TEM) showed a clean crystal structure with the absence of cracks or dislocations in the top 200 nm of the buffer layers. Reciprocal-space mapping (RSM) of the heterostructures around the (335) reciprocal-space point showed a high degree of relaxation (∼95%) of the lower part of the graded buffer. The overall thickness of the compositionally graded buffer was varied depending on the required lattice constant of the topmost layer. To keep grading rates consistent, our grade thicknesses ranged from 2 μm to 3.5 μm for InAsSb with Sb compositions ranging from 20% to 46%. An unstrained 200-nm-thick AlInAsSb carrier confinement layer (virtual substrate) with lattice constant matching the lateral lattice constant of the topmost part of the buffer was grown before the InAsSb layer. The composition of the $InAs_{1-x}Sb_x$ layer was selected to achieve lattice-matching of the confinement layer to the lattice constants of the free-standing (unstrained) InAsSb. The unintentionally doped InAsSb layers were 1 μm thick. The top AlInAsSb confinement layer was similar to the virtual substrate. The heterostructures were capped with a 200-nm-thick InAsSb layer of the same composition as the bulk material to prevent exposure of the Al-containing barrier to the ambient. Details of the growth conditions can be found elsewhere.[18,21]

The design of the type II SLS $InAs_{1-x}Sb_x$/InAs cells was similar to that published in Ref. 19. The InAsSb portions of the SLS period had Sb compositions that were varied in the range from 22.5% to 29.6% by adjusting the Sb/As beam equivalent pressures as presented in Table I. All SLS structures were grown at substrate temperature of 490°C and had target thicknesses of 173 Å and 72 Å, for the InAsSb and InAs layers, respectively. The relatively wide cells were chosen to minimize the energies of the electrons and holes in the SLS. This approach resulted in longer wavelength for the given range of Sb compositions and allowed for more accurate determination of the energy offset at the InAsSb/InAs heterointerface. No AlSb confinement layers were used, in contrast to the design in Ref. 19. The overall thickness of the SLS was 1 μm. The Sb composition was determined by x-ray

Table I. Details of the samples used in PL measurements: wafer number, widths of the InAs and InAsSb layers, composition of Sb in InAsSb, and PL peak energy at $T = 13$ K

Wafer No.	InAs (nm)	InAsSb, Sb %	InAsSb (nm)	Sb/As BEP	Residual Strain (%)	Peak Photon Energy (eV)
K1137	17.0	22.5	7.06	0.133	−0.33	0.191
K1139	17.7	24.2	7.38	0.140	−0.26	0.175
K1140	17.5	25.1	7.30	0.155	−0.22	0.172
K1142	17.5	26.8	7.30	0.170	−0.17	0.152
K1144	17.3	29.6	7.20	0.180	−0.06	0.137

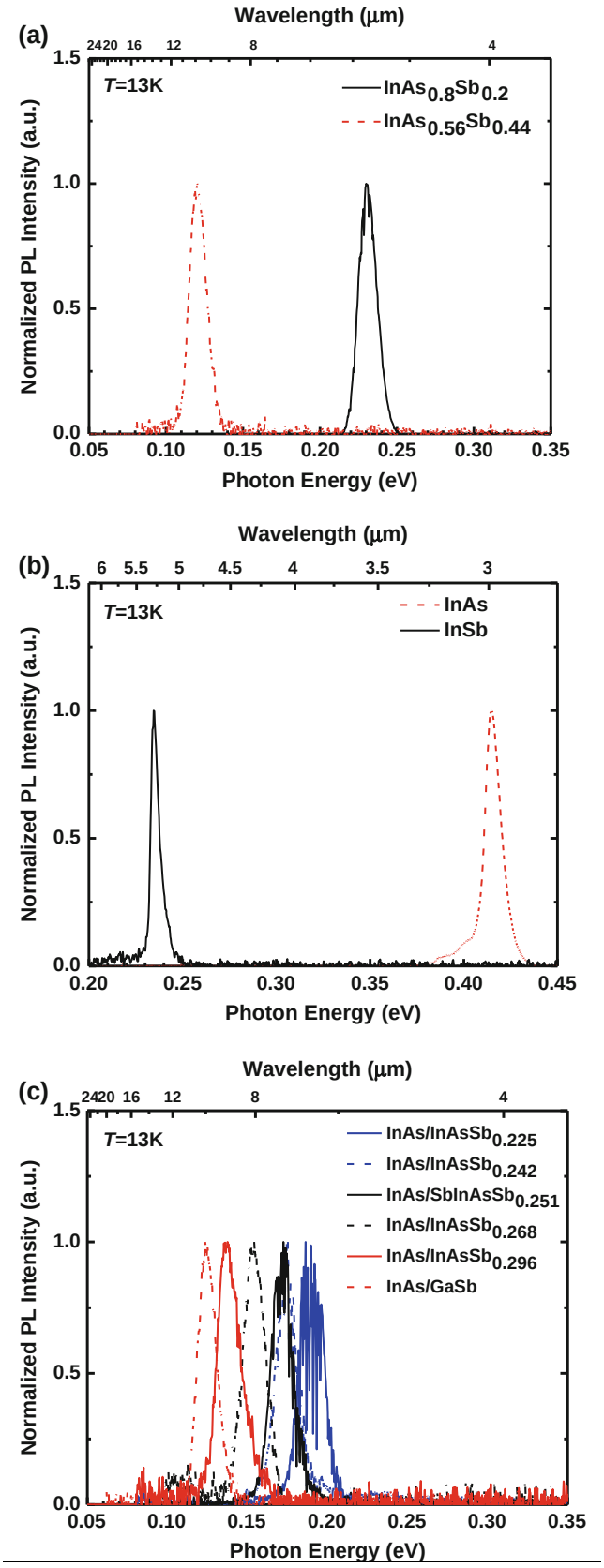

◀ Fig. 1. (a) Normalized PL spectra of bulk $InAs_{0.8}Sb_{0.2}$ and $InAs_{0.56}Sb_{0.44}$. (b) Normalized PL spectra of InAs and InSb layers. (c) Normalized PL spectra of type II InAsSb/InAs SLS with Sb compositions of 22.5%, 24.2%, 25.1%, 26.8%, and 29.6%; the PL spectrum of LWIR InAs/GaSb SLS from Ref. 20 is also shown. The measurements were performed at T = 13 K with excitation power of 100 mW.

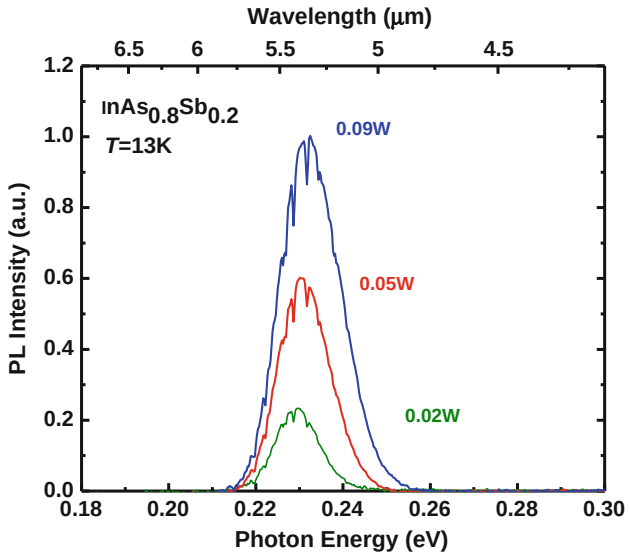

Fig. 2. PL spectra of $InAs_{0.8}Sb_{0.2}$ at T = 13 K measured with excitation power levels of 20 mW, 50 mW, and 90 mW. The excitation area was 1.2×10^{-3} cm^{-2}. The shift of the energy maximum in the range of excitation power was below 2 meV.

diffraction (XRD) fitting. The actual thicknesses of the layers are presented in Table I. Sharp XRD peaks and relatively narrow PL peaks of the samples indicated that the SLS structures were grown under strain of less than 0.33% without relaxation. The 1-μm-thick layers of InAs and InSb were grown on matching substrates to assess the FWHM of the PL spectra of the binary materials for comparison with data for ternary alloys and SLS. The InAs layers were enclosed with carrier confinement layers consisting of several periods of AlSb/AlAs SLS. Details of growth conditions for InAs layers and the design of the confinement layers can be found in Ref. 17.

EXPERIMENTAL PROCEDURES

PL was excited with a Nd:YAG laser (λ = 1064 nm) operating in either continuous-wave (CW) or Q-switched mode. The PL spectra were obtained with a Nicolet Magna-860 Fourier-transform infrared (FTIR) spectrometer. The PL was detected with an external liquid-nitrogen-cooled HgCdTe (MCT) photodetector with spectral response extending up to 14 μm. The excitation source operating in CW mode with external modulation at frequency of 1 kHz and the FTIR spectrometer in step-scan mode were used for PL measurements in the wavelength range longer than 8 μm. In the wavelength range below 8 μm, the FTIR spectrometer was operated in continuous-scan mode. With variation of the sample temperature from 13 K to 300 K, the CW power level ranged from

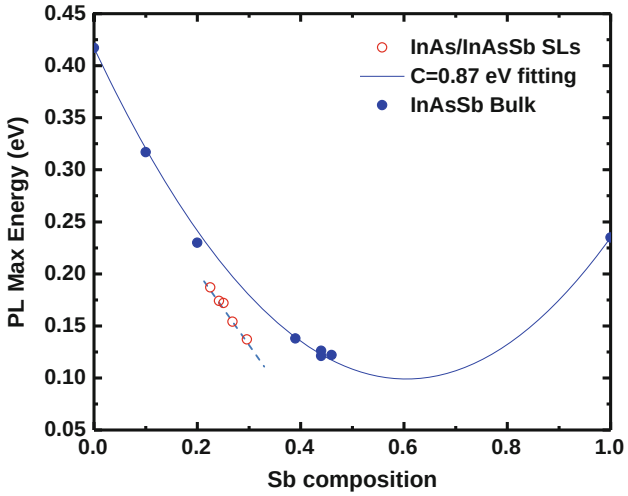

Fig. 3. Dependence of the energy gaps on Sb composition in bulk InAsSb grown on AlInAsSb metamorphic buffers (blue solid circles) and in type II InAsSb/InAs SLS grown on GaSb (red open circles). Data obtained from PL maxima determined at T = 13 K. The fit for bulk InAsSb was obtained with the energy gap bowing parameter of 0.87 eV.

20 mW to 500 mW. The corresponding power densities were from 2 W/cm^2 to 50 W/cm^2. The structures were cooled with a closed-cycle He cryohead M22 (Janis) with ZnSe window coating optimized for high transmission in the long-wavelength infrared range. The PL was collected with the reflective objective. High excitation of SLS structures for population of high-energy states was obtained with the excitation source operating in Q-switched mode with 100-ns pulse width and repetition rate of 100 kHz. The excitation area was 0.5 mm in diameter. The laser emission scattered from the sample and window surfaces was rejected with a Ge filter. The PL spectra measured at several points of the wafers showed high homogeneity of the material composition.

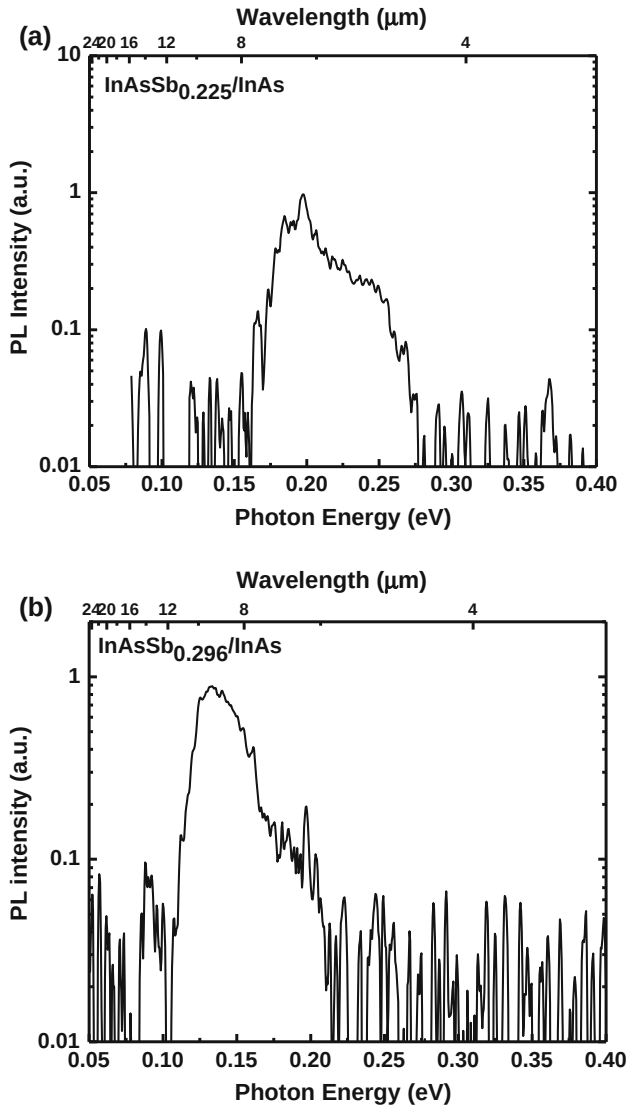

Fig. 4. PL spectra of $InAs_{0.775}Sb_{0.225}$/InAs SLS (a) and $InAs_{0.704}Sb_{0.296}$/InAs SLS (b) under pulsed excitation with pulse width of 100 ns, repetition rate of 100 kHz, and average power of 0.5 W.

RESULTS AND DISCUSSION

The energy gaps were determined from low-temperature PL spectra obtained under low excitation power. This simplified approach provided adequate accuracy for ternary materials. Figure 1 shows the normalized PL spectra of the bulk InAsSb alloys, type II InAsSb/InAs SLS, and binary epilayers measured at T = 13 K. Both the bulk InAsSb materials and type II SLS showed narrow PL spectra with Gaussian line shape. FWHM of 11 meV was measured for the bulk InAsSb layers with both 20% and 44% Sb compositions, being superior to the FWHM values reported for bulk InAsSb grown on AlInAsSb-based SLS buffers.[7] FWHM of about 16 meV was measured for all type II InAsSb/InAs SLS. The FWHM of PL for InAs layers (11 meV) was similar to that for the bulk InAsSb, while the PL spectra of InSb epilayers showed a lower FWHM of 5.5 meV. The FWHM values of InAsSb-based materials measured in this work are comparable to those reported in the literature for longwave infrared (LWIR) InAs/GaSb SLS.[21] Low-temperature PL spectra obtained for a range of excitation powers (Fig. 2) showed that a blue-shift of the PL peak did not exceed 2 meV with increase of CW pumping power from 20 mW to 100 mW. Small values of FWHM of PL spectra at T = 13 K confirmed the good homogeneity of the studied materials. It was concluded that, for measurements of PL spectra in these materials, the pumping power level of 100 mW with excitation area of 10^{-3} cm^2 was adequate.

The energy gaps of the materials were determined from the PL maxima at T = 13 K. The bulk InAsSb layers with 20% and 44% Sb showed peak PL wavelengths of 5.2 μm (E_g = 0.24 eV) and 10.3 μm (E_g = 0.12 eV), respectively. The PL peak wavelengths of type II InAsSb/InAs SLS were in the

range from 6.5 μm (E_g = 0.191 eV) to 9.1 μm (E_g = 0.136 eV) with change of Sb composition in the barrier from 22.5% to 29.6%. The dependences of the energy gap on Sb composition for both bulk and SLS materials are shown in Fig. 3. A number of additional wafers of bulk InAsSb with high Sb compositions were grown after previously reported data.[18] The dependence was fitted using the equation

$$E_{g(\mathrm{InAsSb})} = (1-x)E_{g(\mathrm{InAs})} + xE_{g(\mathrm{InSb})} - x(1-x)C, \quad (1)$$

where $E_{g(\mathrm{InAsSb})}$, $E_{g(\mathrm{InAs})}$, and $E_{g(\mathrm{InSb})}$ are the energy bandgaps of the materials and C is the bowing parameter for the energy gap. A good fit was obtained for C = 0.87 eV. The obtained value was greater than that reported in most experimental works and greater than the previously recommended value of 0.67 eV.[22] The variations in the reported data could be explained by differences in the growth conditions or the presence of residual strain of various degrees in the reported data, which can affect the energy band spectra and may lead to the possibility of Cu-Pt ordering.[7,23]

The energy gaps for InAsSb/InAs SLS are lower than those for bulk InAsSb with similar Sb compositions due to the type IIc band line-up.[8] In Fig. 3, one can see a trend of more rapidly decreasing bandgaps for the SLS than the bulk material for increasing Sb composition. This implies that the band offsets, ΔE_c, must be increasing with the Sb composition at a faster rate than the InAsSb bandgap itself. We can quantify the relative band positions as follows: Considering the relatively low conduction-band offsets in InAsSb/InAs SLS structures, high-energy states in the conduction band of InAs can be populated with electrons, revealing details of the energy structure of the SLS from PL spectra. Experimentally, this approach was implemented with higher-energy pulsed excitation using the solid-state laser operating in Q-switched mode. Population of high-energy states under pulsed excitation of carriers in $InAs_{1-x}Sb_x$/InAs SLS resulted in broadening of the PL spectra. Under low excitation, only a single PL peak was observed (Fig. 1). For the InAsSb/InAs SLS structure with 22.5% Sb the main peak was centered at photon energy of 0.19 eV and the second peak was observed at 0.25 eV (Fig. 4a). We associated the second PL peaks with the transitions of electrons from the 3D continuum to quasi-2D hole states in the InAsSb portion of the SLS period. The peak energy differences of 60 meV can be interpreted as the distance from the bottom of the SLS miniband to the bottom of the conduction band in the $InAs_{0.775}Sb_{0.225}$ barriers.

Calculation of low-temperature energies was performed using the material parameters recommended in Ref. 22. The energy gap bowing parameter was taken to be 0.87 eV as obtained in this work. The stiffness coefficients C_{11} and C_{12} as well as the deformation coefficients for the conduction band (a_c) and valence band (a_v and b) for binaries were taken from Ref. 22 as follows: for InSb: a_c = −6.94 eV, a_v = −0.36 eV, b = −2.0 eV, C_{11} = 684.7 GPa, and C_{12} = 373.5 GPa; for InAs: a_c = −5.08 eV, a_v = −1.0 eV, b = −1.8 eV, C_{11} = 832.9 GPa, and C_{12} = 452.6 GPa. In Fig. 5, for free-standing $InAsSb_{0.225}$ with lattice constant of 6.147 Å the following coefficients were obtained by linear interpolation of the data for binaries: a_c = −5.5 eV, a_v = −0.856 eV, b = −1.845 eV, C_{11} = 800 GPa, and C_{12} = 435 GPa. The in-plane strain in $InAsSb_{0.225}$ grown on GaSb was calculated to be ε = −1.05%. In accordance with Ref. 29, the shifts of the conduction- and valence-band energies due to hydrostatic strain were calculated as $\delta H_c = 2a_c(1 - C_{12}/C_{11})\varepsilon$ = 51 meV and $\delta H_v = -2a_v(1 - C_{12}/C_{11})\varepsilon$ = −8 meV, respectively. The split of hole energy into subbands due to the shear strain was found to be $\delta S = b(1 + 2C_{12}/C_{11})\varepsilon$ = 39 meV. The overall shifts of the heavy- and light-hole energies were found to be δE_{hh} = 31 meV and δE_{lh} = −47 meV, respectively. The miniband energies in SLS estimated by the Kronig–Penney model were relatively small, playing a minor role compared with the effects of strain. First, the valence-band energy for InAsSb of a given Sb composition was obtained from linear interpolation between E_v = −590 meV in InAs and E_v = 0 meV in InSb. For InAsSb with 22.5% Sb grown on GaSb, an unstrained valence-band energy of E_v = −457 meV was obtained. For the 1.1% compressive strain in the growth direction

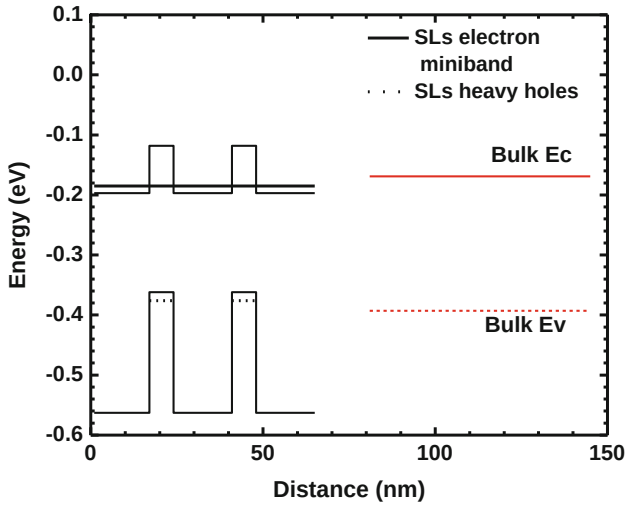

Fig. 5. Band profile of two-period InAs/$InAs_{0.775}Sb_{0.225}$. The black solid line represents the miniband energy position. The black dotted lines represent the energy position of heavy holes. The red lines represent the energy position of the conduction band of free-standing $InAs_{0.775}Sb_{0.225}$. The red dotted lines represent the energy position of the valence band of free-standing $InAs_{0.775}Sb_{0.225}$. The energy position of the miniband is 12 meV above the conduction band of InAs. The energy position of the heavy holes is 14 meV below the valence band of $InAs_{0.775}Sb_{0.225}$.

calculated for $InAs_{0.775}Sb_{0.225}$ on GaSb, the hole splitting and energy shift would result in a heavy-hole energy of $E_{hh} = -426$ meV. The hole miniband energy with respect to the edge was estimated to be 14 meV. This resulted in a maximum hole energy in $InAs_{0.775}Sb_{0.225}$ of $E_h = -440$ meV. For free-standing InAs the conduction-band energy was taken to be $E_c = -173$ meV. For InAs on GaSb substrate at $T = 13$ K, tensile strain of -0.57% was obtained. Accounting for strain resulted in electron energy of $E_c = -197$ meV. The energy of the bottom of the electron miniband was estimated to be 12 meV. The minimum electron energy in InAsSb/InAs SLS was estimated to be $E_e = -185$ meV. Thus, linear interpolation of the valence-band energy predicted an SLS energy gap of 255 meV, while the experiment suggested E_g of 191 meV. To obtain matching with the experiment, a 64 meV difference was added to the valence-band energy of $InAs_{0.775}Sb_{0.225}$.

The conduction-band energy in $InAs_{0.775}Sb_{0.225}$ was corrected accordingly, resulting in an increase of the conduction-band offset. For free-standing material, $E_c = -169$ meV was obtained. Accounting for strain resulted in $E_c = -118$ meV. Thus, the energy barrier for electrons was estimated to be 67 meV, which is reasonably close to the value of 60 meV obtained from interpretation of the experiment.

For InAsSb with 29.6% Sb, an electron barrier of 88 meV was predicted. Due to the large value of the barrier, for this structure the second peak in the broadened PL spectra was not observed (Fig. 4b). For the SLS sample with Sb composition of 25.1% the shape of the broadened PL spectra

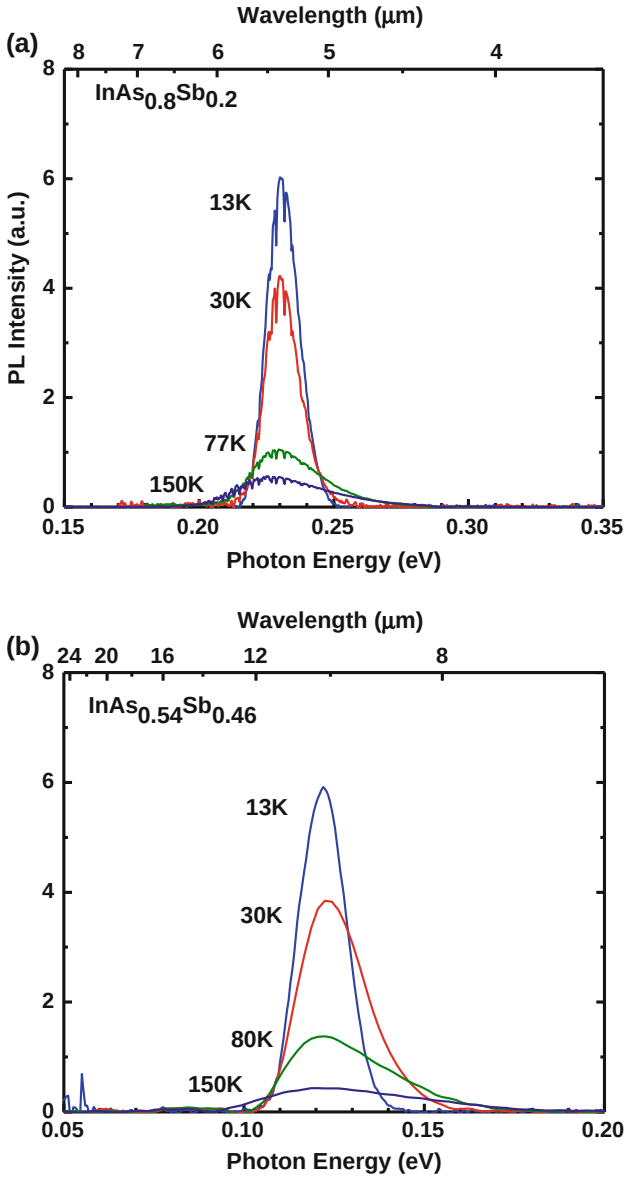

Fig. 6. PL spectra of bulk $InAs_{0.8}Sb_{0.2}$ (a) and $InAs_{0.54}Sb_{0.46}$ (b) at $T = 13$ K, 30 K, 77 K, and 150 K. Excitation power was 100 mW.

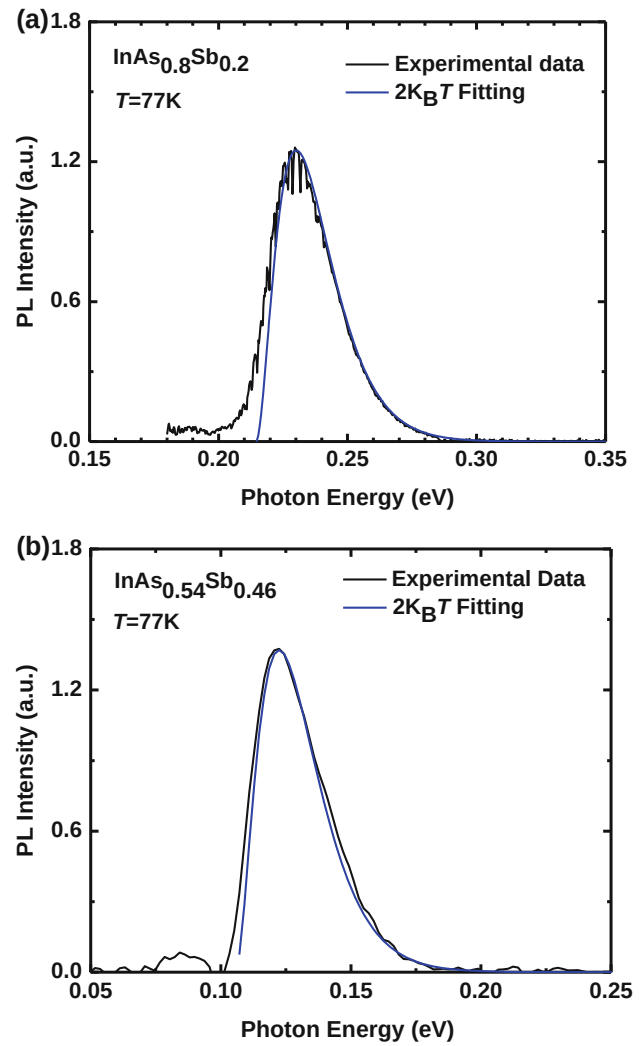

Fig. 7. PL spectra of bulk $InAs_{0.8}Sb_{0.2}$ (a) and $InAs_{0.56}Sb_{0.46}$ (b) at $T = 77$ K (black lines) and fitting based on Eq. 3 (blue lines). See the text for details on fitting.

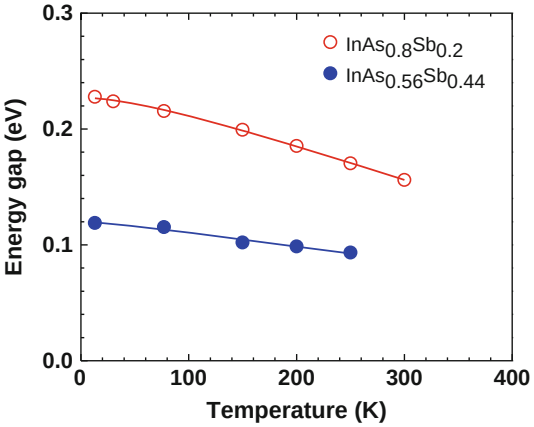

Fig. 8. Temperature dependences of the energy gaps of bulk $InAs_{0.8}Sb_{0.2}$ (a) and $InAs_{0.56}Sb_{0.44}$ (b). The fits were obtained using the following Varshni parameters: E_{g0} = 0.226 eV, α = 3.2 meV/K, and b = 100.4 K for $InAs_{0.8}Sb_{0.2}$; E_{g0} = 0.119 eV, α = 1.2 meV/K, and b = 33.3 K for $InAs_{0.56}Sb_{0.44}$.

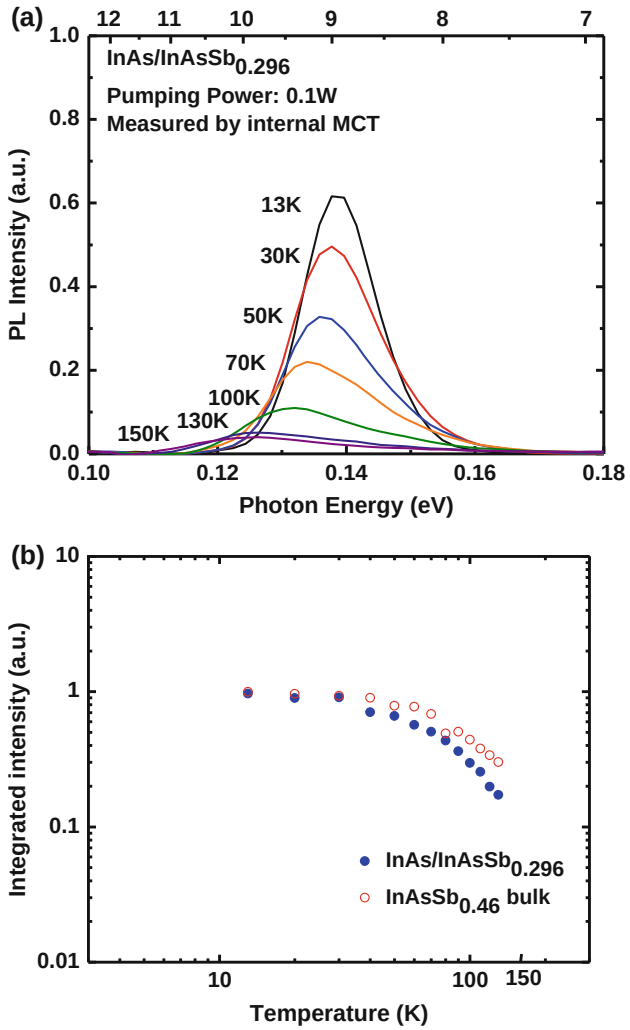

Fig. 9. (a) PL spectra of InAsSb/InAs with Sb composition of 29.6% in the temperature range from 13 K to 150 K. (b) Temperature dependences of integrated PL intensities obtained from data for type II InAsSb/InAs SLS and for bulk $InAs_{0.54}Sb_{0.46}$. Excitation power was 100 mW.

was influenced by the absorption of vapors in the atmosphere.

The energy estimations above are based on several assumptions which contain uncertainties, beginning with the position of the InAs E_v relative to that of InSb and the effect of strain. Note, for example, that the strain effect is entirely responsible for moving the InAsSb bands from a type I to a type IIc line-up with the InAs.

The obtained results suggest negative bowing for the valence-band energy of InAsSb. Adopting the constant bowing parameter results in a value of −0.3 eV for the valence band for Sb composition in the range from 20% to 30%, which is in agreement with the results of Ref. 10. With extrapolation of the dependence to lower Sb compositions, a larger bowing parameter would be expected. This observation is in agreement with the results presented in Ref. 9. Extrapolation to larger Sb composition would result in smaller bowing parameters. The latter was confirmed in Ref. 24 in a study of SLS with higher Sb compositions. The assumption of a value of −0.3 eV for the valence-band bowing leaves a value of +0.57 eV for the bowing parameter of the conduction band.

The temperature dependences of the energy gaps were determined with the help of PL spectra. The PL spectra of bulk InAsSb for both Sb compositions in the temperature range up to 150 K were measured under a constant excitation level of 100 mW (Fig. 6). In this range, the bulk $InAs_{0.8}Sb_{0.2}$ showed a 30 meV shift of the PL peak, while for $InAs_{0.54}Sb_{0.46}$ the energy was nearly constant. To determine the energy gap from the PL spectra, we must account for the broadening of PL with temperature. Assuming conservation of the wavevector in direct-bandgap recombination with photon emission, one can expect the line shape of the PL spectrum to be described by the following expression:[25]

$$I(h\omega) \propto (h\omega - E_g)^{1/2} \exp(-(h\omega - E_g)/k_B T), \quad (2)$$

where $h\omega$ is the photon energy, E_g is the energy bandgap of the material, k_B is the Boltzmann constant, and T is the temperature of carriers. By differentiation of Eq. 2 one can show that the PL emission achieves its peak at photon energy of $k_B T/2$ greater than the energy of the bandgap. Thus, with wavevector conservation in the PL process, the energy gap can be estimated by subtraction of a half of $k_B T$ from the photon energy at the peak PL value.

In the experiment, the high-energy tail in the PL spectrum can be fitted by an exponential term in expression (2) while in the range to the left of the PL maximum the line shape is broader than that predicted by Eq. 2. Following the approach often used in literature,[6,26] the expression for fitting of the

experimental spectra was taken as shown below with a $(h\omega - E_g)$ term to power n:

$$I(h\omega) \propto (h\omega - E_g)^n \exp(-(h\omega - E_g)/k_B T). \quad (3)$$

Figure 7 shows the fits to the PL spectra obtained with the use of Eq. 3. A good fit of the experimental data was obtained with n close to 2. The value $n = 2$ can be justified for the case of radiative recombination without conservation of the wavevector.[26] Thus, the experimental results obtained in this work suggest participation of phonons in the radiative recombination process. Deviation from the fit at low energies could be explained by a contribution from weaker, two-phonon processes. With $n = 2$ the energy gap can be obtained by subtraction of $2k_BT$ from the PL maxima. Note that, for InAsSb with 46% Sb composition, the value of $2k_BT$ is about 10% of the energy bandgap at 77 K. Figure 8 shows the temperature dependence of the energy gap obtained from the PL maximum by subtraction of $2k_BT$. The dependences were fitted using the Varshni parameters shown below:[27]

$$E_g = E_{g0} - \alpha T^2/(T + \beta), \quad (4)$$

where E_{g0} represents the energy gap of the material at $T = 0$ K. The best fits were obtained with $\alpha = 0.32$ meV/K, $\beta = 100.4$ K and $\alpha = 0.12$ meV/K, $\beta = 33.3$ K for bulk $InAs_{0.80}Sb_{0.20}$ and $InAs_{0.56}Sb_{0.44}$, respectively. The empirical parameter β is often attributed to the Debye temperature.[28] A smaller β value for $InAs_{0.54}Sb_{0.46}$ implies a greater role of lattice vibrations in narrow-gap materials. This may explain a greater role of radiative recombination without wavevector conservation in the PL of narrow-gap materials.

The temperature dependences of the PL intensities and energies of the PL maxima in $InAs_{0.704}Sb_{0.296}$/InAs SLS in comparison with bulk $InAs_{0.54}Sb_{0.46}$ are shown in Fig. 9. The data suggest that the PL intensities of the bulk and SLS materials are comparable in the low-temperature range ($T < 30$ K). Outside of this range, the PL intensity of the bulk materials decreases more slowly with temperature compared with that of the SLS. The peak PL energy of the bulk material is less sensitive to temperature. A weak temperature dependence of the PL peak for $InAs_{0.56}Sb_{0.46}$ was mentioned above. For the InAsSb/InAs SLS, in addition to the effect of the stronger temperature dependence of the energy gap in InAs, the energy of radiative transitions depends also on the temperature dependence of the band offset. The temperature dependence of the energy gap in $InAs_{0.704}Sb_{0.296}$/InAs SLS was fitted using Varshni parameters of $\alpha = 0.18$ meV/K and $\beta = 135$ K, similar to those reported in Ref. 12.

CONCLUSIONS

Temperature dependences of PL spectra were obtained for unrelaxed bulk InAsSb and type II InAsSb/InAs with Sb compositions corresponding to energy gaps in the midwave and longwave infrared spectral ranges. Low-temperature energy gaps as low as 0.120 eV and 0.136 eV with PL FWHM of 11 meV and 16 meV were demonstrated for bulk InAsSb and type II InAsSb/InAs, respectively. The bowing parameter for bulk InAsSb was found to be 0.87 eV, considerably greater than the previously recommended value of 0.67 eV. The experimental data on the conduction-band offset at the $InAs_{0.775}Sb_{0.225}$/InAs interface suggest bowing parameters for the conduction and valence bands of +0.57 eV and −0.3 eV, respectively. This result is based on the assumption of 0.59 eV difference between the valence-band energies of InAs and InSb. Broadening of PL spectra with temperature was attributed to phonon-assisted radiative recombination without wavevector conservation.

ACKNOWLEDGEMENTS

The work was supported by NSF Grant DMR1160843 and Army Research Office Contract 62447EL.

REFERENCES

1. A.G. Thompson and J.C. Woolley, *Can. J. Phys.* 45, 2597 (1967).
2. G.C. Osbourn, *J. Vac. Sci. Technol. B* 2, 176 (1984).
3. G.S. Lee, Y. Lo, Y. F. Lin, S. M. Bedair, W. D. Laidig. *Appl. Phys. Lett.* 47, 1219 (1985).
4. L.R. Dawson, *J. Vac. Sci. Technol. B* 4, 598 (1986).
5. M.Y. Yen, B.F. Levine, C.G. Bethea, K.K. Choi, and A.Y. Cho, *Appl. Phys. Lett.* 50, 927 (1987).
6. Z.M. Fang, K.Y. Ma, D.H. Jaw, R.M. Cohen, and G.B. Stringfellow, *J. Appl. Phys.* 67, 7034 (1990).
7. S.R. Kurtz, L.R. Dawson, R.M. Biefeld, D.M. Follstaedt, and B.L. Doyle, *Phys. Rev. B* 46, 1909 (1992).
8. S.-H. Wei and A. Zunger, *Phys. Rev. B.* 52, 12039 (1995).
9. P.-W. Liu, G. Tsai, H.H. Lin, A. Krier, Q.D. Zhuang, and M. Stone, *Appl. Phys. Lett.* 89, 201115 (2006).
10. D. Lackner, O.J. Pitts, M. Steger, A. Yang, M.L.W. Thewalt, and S.P. Watkins, *Appl. Phys. Lett.* 95, 081906 (2009).
11. D. Lackner, O.J. Pitts, S. Najmi, P. Sandhua, K.L. Kavanagha, A. Yang, M. Steger, M.L.W. Thewalt, Y. Wang, D.W. McComb, C.R. Bolognesi, and S.P. Watkins, *J. Cryst. Growth* 311, 3563 (2009).
12. E.H. Steenbergen, Y. Huang, J.H. Ryou, R.D. Dupuis, K. Nunna, D.L. Huffaker, and Y.-H. Zhang, *AIP Conf. Proc.* 1416, 122 (2011).
13. E.H. Steenbergen, Y. Huang, J.-H. Ryou, L. Ouyang, J–.J. Li, D.J. Smith, R.D. Dupuis, and Y.-H. Zhang, *Appl. Phys. Lett.* 99, 071111 (2011).
14. L. Ouyang, E.H. Steenbergen, O.O. Cellek, Y.-H. Zhang, and D.J. Smith, *Proc. SPIE.* 8268, 826830 (2012).
15. E.H. Steenbergen, K. Nunna, L. Ouyang, B. Ullrich, D.L. Huffaker, and Y.-H. Zhang, *J. Vac. Sci. Technol. B.* 30, 02B107 (2012).
16. D. Lackner, M. Steger, M.L.W. Thewalt, O.J. Pitts, Y.T. Cherng, S.P. Watkins, E. Plis, and S. Krishna, *J. Appl. Phys.* 111, 034507 (2012).
17. S.P. Svensson, D. Donetsky, D. Wang, H. Hier, F.J. Crowne, and G. Belenky, *J. Cryst. Growth* 334, 103 (2011).

18. G. Belenky, D. Donetsky, G. Kipshidze, D. Wang, L. Shterengas, W.L. Sarney, and S.P. Svensson, *Appl. Phys. Lett.* 99, 141116 (2011).
19. E.H. Steenbergen, B.C. Connelly, G.D. Metcalfe, H. Shen, M. Wraback, D. Lubyshev, Y. Qiu, J.M. Fastenau, A.W.K. Liu, S. Elhamri, O.O. Cellek, and Y.-H. Zhang, *Appl. Phys. Lett.* 99, 251110 (2011).
20. B.V. Olson, E.A. Shaner, J.K. Kim, J.F. Klem, S.D. Hawkins, L.M. Murray, J.P. Prineas, M.E. Flatte, and T.F. Boggess, *Appl. Phys. Lett.* 101, 092109 (2012).
21. D. Wang, Y. Lin, D. Donetsky, L. Shterengas, G. Kipshidze, G. Belenky, W.L. Sarney, H. Hier, and S.P. Svensson, *Proc. SPIE.* 8353, 835312 (2012).
22. I. Vurgaftman, J.R. Meyer, and L.R. Ram-Mohan, *J. Appl. Phys.* 89, 5815 (2001).
23. S.P. Svensson, W.L. Sarney, H. Hier, Y. Lin, D. Wang, D. Donetsky, L. Shterengas, G. Kipshidze, and G. Belenky, BV11776, *Phys. Rev.* B.
24. E.H. Steenbergen, O.O. Cellek, D. Lubyshev, Y. Qiu, J.M. Fastenau, A.W.K. Liu, Y.-H. Zhang, *Proc. SPIE.* 8268, 82680K9 (2012).
25. H.B. Bebb and E.W. Williams, in *Semiconductors and Semimetals*, ed. by R.K. Willardson and A.C. Beer (Academic, New York, London, 1972), Vol. 8, Ch. 4, p. 238.
26. A.T. Hunter and T.C. McGill, *J. Appl. Phys.* 52, 5779 (1982).
27. Y.P. Varshni, *Physica.* 34, 149 (1967).
28. H.C. Casey Jr and M.B. Panish, *Heterostructure Lasers* (Academic, New York, 1978), 2, 9–10.
29. S.L. Chuang, *Phys. Rev. B* 43, 9649 (1991).